HIV-1 Cell to Cell Transfer across an Env-induced, Actin-dependent Synapse

Clare Jolly,[1] Kirk Kashefi,[2] Michael Hollinshead,[3] and Quentin J. Sattentau[2]

[1]*The Sir William Dunn School of Pathology, The University of Oxford, Oxford OX1 3RE, UK*
[2]*The Jefferiss Trust Laboratories and* [3]*The Henry Wellcome Imaging Suite, The Wright-Fleming Institute, Imperial College Faculty of Medicine, London W2 1PG, UK*

Abstract

Direct cell–cell transfer is an efficient mechanism of viral dissemination within an infected host, and human immunodeficiency virus 1 (HIV-1) can exploit this mode of spread. Receptor recognition by HIV-1 occurs via interactions between the viral surface envelope glycoprotein (Env), gp120, and CD4 and a chemokine receptor, CCR5 or CXCR4. Here, we demonstrate that the binding of CXCR4-using HIV-1–infected effector T cells to primary CD4$^+$/CXCR4$^+$ target T cells results in rapid recruitment to the interface of CD4, CXCR4, talin, and lymphocyte function–associated antigen 1 on the target cell, and of Env and Gag on the effector cell. Recruitment of these membrane molecules into polarized clusters was dependent on Env engagement of CD4 and CXCR4 and required remodelling of the actin cytoskeleton. Transfer of Gag from effector to target cell was observed by 1 h after conjugate formation, was independent of cell–cell fusion, and was probably mediated by directed virion fusion with the target cell. We propose that receptor engagement by Env directs the rapid, actin-dependent recruitment of HIV receptors and adhesion molecules to the interface, resulting in a stable adhesive junction across which HIV infects the target cell.

Key words: CD4 • CXCR4 • cytoskeleton • T cells • adhesion molecules

Introduction

Viruses can disseminate within an infected host by two mechanisms: (a) release of cell-free virions and (b) direct passage between infected and uninfected cells. In general, direct cell–cell transfer is more rapid and efficient than cell-free spread because it obviates rate-limiting early steps in the virus life cycle, such as virion attachment (1). Moreover, cell–cell passage may help viruses evade elements of the immune response, such as neutralizing antibodies and complement. For viruses such as the human T cell leukemia virus type 1 (HTLV-1), cell–cell infection appears to be the principal mode of dissemination within and between hosts (2). HIV-1 can spread by cell-free virus and via direct cell–cell transmission (1, 3). The relative contribution of these two modes of HIV-1 dissemination in vivo is not established, but cell–cell spread is probably an important mechanism in tissues densely populated with target cells, such as CD4$^+$ T cells in lymph nodes (4).

In vitro systems have been established to study cell–cell spread of HIV-1 between various cell types. These include virus transfer between infected and uninfected immortalized CD4$^+$ T cell lines (5, 6); between infected CD4$^+$ T cells and epithelial cells (7); between infected macrophages and epithelial cells (8) and CD4$^+$ T cells (8); and between virus-pulsed dendritic cells and CD4$^+$ T cells (9–11). Several papers have addressed the rate of new proviral DNA synthesis after cell–cell infection (5, 12); incoming HIV-1 RNA is reverse transcribed, and new virus is produced considerably faster than after cell-free virus infection. Cell–cell transfer of HIV-1 has been visualized in conjugates of infected and uninfected cells by fluorescence (11) and electron microscopy (1, 3). Virus budding polarizes on infected cells, and the polar cap of viral egress is frequently directed toward the site of contact with the target cell (1, 3, 11).

Cells permissive for HIV-1 infection express CD4 and a chemokine receptor (CKR), either or both of CCR5 and CXCR4 (13). HIV-1 virions or HIV-1–infected cells bind these receptors via the viral surface envelope glycoprotein (Env) subunit, gp120. The ligation of CD4 by gp120 triggers

Address correspondence to Quentin J. Sattentau, The Sir William Dunn School of Pathology, University of Oxford, South Parks Road, Oxford OX1 3RE, UK. Phone: 01-86-52-75-511; Fax: 01-86-52-75-515; email: quentin.sattentau@pathology.ox.ac.uk

conformational changes in Env that expose a binding surface for the CKR on gp120 (14). Subsequent interactions between gp120 and the CKR activate the Env transmembrane glycoprotein, gp41, which fuses the Env-containing membrane with the receptor-expressing target cell membrane. Membrane fusion by cell-free virus transfers the viral core into the target cell cytoplasm, initiating the intracellular portion of the virus life cycle. HIV-1–mediated fusion is generally considered a relatively simple, two-step process. However, a greater level of complexity arises from the requirement for more than one CD4 molecule to interact with each Env trimer (15, 16) and for multiple Env–receptor complexes to form a fusion pore (17, 18). Moreover, some recent studies have hinted that HIV-induced fusion may involve recruitment of elements of the actin cytoskeleton within the target cell (19, 20).

HIV-1–Env-receptor interactions have been studied very little in a membrane context. Models of HIV-1 cell–cell fusion have provided insight into the requirements and rate of Env-mediated membrane fusion (21–23), but do not directly address the movement of Env and receptors in their respective membranes. To investigate the membrane dynamics of the HIV-1 receptors during Env engagement and the potential role of the actin cytoskeleton in cell–cell infection, we established a system to analyze events at the interface between HIV-1–infected and receptor-expressing T cells. Using this system, we demonstrate that receptor engagement by Env triggers rapid, actin-dependent recruitment of CD4, CXCR4, and LFA-1 on the target cell and Env-Gag coclustering in the effector cell, followed by transfer of viral Gag into the target cell. We propose that HIV-1 induces in CD4$^+$ T cells a stable adhesive junction, or synapse, containing multiple Env–receptor complexes and adhesion molecules, facilitating rapid and efficient infection of the target cell.

Materials and Methods

Cells and Tissue Culture. The CD4$^+$/CXCR4$^+$ T cell line Jurkat CE6.1 (American Type Culture Collection) and the CD4$^+$/CXCR4$^+$ T cell line A3.01 (The Centralized Facility for AIDS Reagents [CFAR]) were maintained in suspension cell growth medium (RPMI 1640 [GIBCO BRL] supplemented with 100 U/ml penicillin, 100 μg/ml streptomycin, and 5% FCS). PBMCs were separated from fresh blood of a healthy HIV-1–seronegative donor using a Ficoll-Hypaque gradient and negatively enriched for CD4$^+$ T cells by magnetic cell sorting according to the manufacturer's instructions (Miltenyi Biotec). Cells were diluted in RPMI 1640–1% FCS (wash buffer [WB]) and used immediately. Flow cytometric analysis of the cells by indirect immunofluorescence using mAbs to CD4 (Q4120; CFAR; reference 24) and CD3 (UCHT1, obtained from P. Beverley, Jenner Institute for Vaccine Research, Compton, UK) established that they were routinely >90% pure CD4$^+$ T cells (hereafter target cells). Effector cells were Jurkat CE6.1 chronically infected with the T cell line–adapted HIV-1 strain LAI (Jurkat$_{LAI}$). 5 × 10^6 Jurkat cells were infected at a multiplicity of infection of 0.01 and cultured for 7 d. Cells were phenotyped for surface Env expression using pooled human anti-HIV immunoglobulin (AIDS Research and Reference Reagent Program,) at 50 μg/ml, detected by anti–human-IgG–phycoerythrin (Jackson ImmunoResearch Laboratories) and for CD4 expression using mAb L120 (24) obtained from the CFAR. Cells were used from days 7 to 14 after infection when Env expression was readily detectable and CD4 expression was negative.

Conjugate Formation, Immunostaining, and Confocal Microscopy. 5 × 10^5 effector cells were diluted in WB and mixed with an equal number of target cells at 37°C on poly-L-lysine (Sigma-Aldrich)–treated coverslips for up to 360 min with or without the inclusion of mAb. Conjugate evolution was arrested on ice, and cells were fixed in 4% formaldehyde in PBS-1% BSA for 15 min at 4°C or in prechilled methanol for 5 min at room temperature (RT). Surface staining of cells after conjugate formation was performed on ice in buffer containing 0.05% NaN$_3$ before fixing with formaldehyde. For intracellular staining of actin, talin, and HIV-1 Gag, conjugates were fixed and permeabilized in 0.1% Triton X-100/5% FCS. For kinetic studies, conjugate formation was synchronized by mixing effector with target cells and incubating on coverslips at 4°C for 30 min before transferring to 37°C. Immunostaining of conjugates was performed using the following mAbs: gp41-specific, CD4-induced mAb 50-69 (CFAR; reference 25), CD4 (L120), and CXCR4 (6H8; reference 26). In dual staining experiments, CXCR4 was detected with 12G5-FITC (R&D Systems) after staining with L120 and the anti–mouse Fab secondary antibody, followed by quenching with normal mouse serum. Rabbit antisera against HIV-1 Gag p17 and p24 were obtained from the CFAR. Talin was detected with murine mAb 8D4 (Sigma-Aldrich), LFA-1 with the murine mAb HI111 (BD Biosciences) and actin with phalloidin-TRITC (Sigma-Aldrich). Primary antibodies were visualized by single, double, and triple color staining using FITC, TRITC, or Cy5-conjugated donkey anti–human, mouse, rat, or rabbit IgG F(ab′)$_2$, or streptavidin-Cy5 reagents tested for absence of interspecies cross-reactivity (Jackson ImmunoResearch Laboratories). Stained coverslips were mounted in Molwiol 4-88 (Calbiochem), and analyzed using a META™ confocal microscope linked to LSM 510™ software (Carl Zeiss MicroImaging, Inc.). Images were acquired sequentially using the multitrack configuration of the Zeiss META™ to avoid cross-talk between fluorescence channels, and the appropriate controls with and without primary antibody were performed. Additional image processing was performed using Adobe Photoshop 7, and images are presented as single two-dimensional x-y sections and the corresponding Nomarski image unless otherwise stated.

Inhibition of Cytoskeletal Rearrangement and Signaling. Target cells were treated with 1 μM cytochalasin D (Sigma-Aldrich), jasplakinolide, or latrunculin-A (Molecular Probes) in suspension cell growth medium at 37°C for 60 min before conjugate formation. Myosin motor function was inhibited by pretreating cells with 20 mM butane-dione monoxime (BDM; Sigma-Aldrich) for 30 min at 37°C or 20 μM ML7 (Calbiochem) for 60 min at 37°C. Myosin motor protein kinase was inhibited by pretreatment of cells with 100 nM wortmannin (Tocris) at 37°C for 30 min. Inhibitor was removed by washing the treated cells in WB just before conjugate formation. To block Env–CD4 and Env–CXCR4 interactions, target cells were incubated with 10 μg/ml of Q4120 or AMD3100 (obtained from J. Moore, Cornell University, New York, NY) or effector cells with 447D-52D (obtained from S. Zolla-Pazner, National Institutes of Health Repository, Bethesda, MD) (27) for 30 min at 37°C before conjugate formation.

Conjugate Quantification and Statistical Analysis. Conjugates were prepared and analyzed as aforementioned, and multiple, random sections of low-power fields were acquired. The total

number of target cells was counted, and the percentage of target cells within conjugates was quantified. Conjugates were defined as closely apposed pairs of cells containing at least one CD4+ and one Env+ cell. Each conjugate was analyzed for polarization of Env or a target cell marker, or for intracellular staining of actin, talin, or Gag. Results are presented as percentage of target cells within conjugates, and the percentage of conjugates containing staining polarized to the interface, and are representative of at least two independent experiments. Statistical analysis on the median values of conjugate counts was performed using a paired, two-tailed Student's *t* test.

Cell–Cell Fusion Assay. 5×10^6 effector and target cells were labeled with the cytoplasmic dyes CellTracker orange CMTMR and CellTracker green CMFDA, respectively (Molecular Probes), according to manufacturer's instructions. Labeled cells were washed extensively, mixed, and seeded onto polylysine coverslips for up to 24 h at 37°C, with or without 10 μg/ml of the peptide DP178 (28) obtained from T. Matthews (University of Alabama, Birmingham, Birmingham, AL). Cells were fixed in formaldehyde and analyzed by confocal microscopy.

Transmission Electron Microscopy (TEM). 2×10^6 effector cells were mixed with an equal number of target cells, gently sedimented by low-speed centrifugation and conjugates formed at 37°C for 1 h in the presence of 5 μg/ml L120. Excess buffer was removed, and cells were gently resuspended in 250 mM Hepes buffer containing 4% paraformaldehyde for 10 min on ice followed by 8% paraformaldehyde for 50 min at RT. After washing in PBS-5% FCS and quenching with 50 mM NH_4Cl_2, cells were incubated with rabbit anti–mouse IgG for 1 h and labeled with 6 nm protein A gold particles for 2 h. The cells were fixed for 30 min in 200 mM cacodylate and 0.5% glutaraldehyde. All incubations were performed at RT, and cells were washed extensively in PBS-5% FCS between steps. Samples were washed in 200 mM cacodylate and post-fixed in 1% osmium tetroxide and 1.5% potassium ferrocyanide for 1 h. After extensive washing in water, cells were incubated in 0.5% magnesium uranyl acetate overnight at 4°C, dehydrated in ethanol and propylene oxide, and embedded in epon resin. Ultrathin sections were cut and collected on TEM grids, and lead citrate was added as a contrast agent. Sections were analyzed using an FEI Technai G2 transmission electron microscope, and digital images were captured using Soft Imaging Software and processed in Adobe Photoshop 7.

Results

Recruitment of HIV-1 Receptors to the Effector–Target Cell Interface.   To study movement of viral receptors in the context of cell–cell HIV-1 infection, we established a system based on the formation of conjugates between the Jurkat T cell line chronically infected with an X4 HIV-1 virus isolate (LAI), termed Jurkat$_{LAI}$ (effector cells), and CD4+ T cells (target cells) enriched by >90% by negative selection from PBMCs. Conjugates were formed at 37°C in the presence or absence of antibodies. Fusion was arrested on ice, and conjugates were fixed, stained, and analyzed by confocal microscopy. Because HIV-1–infected Jurkat cells down–regulate CD4 concomitant with the expression of HIV-1 Env, staining for Env and CD4 allows unequivocal differentiation of effector from target cells. In most experiments, cells were stained during conjugate formation with two mAbs that are noninhibitory for Env–receptor interac-

tions and Env-mediated fusion: the CD4-specific mAb L120 and the gp41-specific mAb 50-69. In initial experiments, these mAbs were added after conjugate formation; identical results were obtained in both cases.

Low-power analysis of conjugates incubated for 10–60 min at 37°C in the presence of L120 and 50-69 revealed coclustering of CD4 and Env at the interface of effector–target cell conjugates. Fig. 1 A shows a typical low-power field in
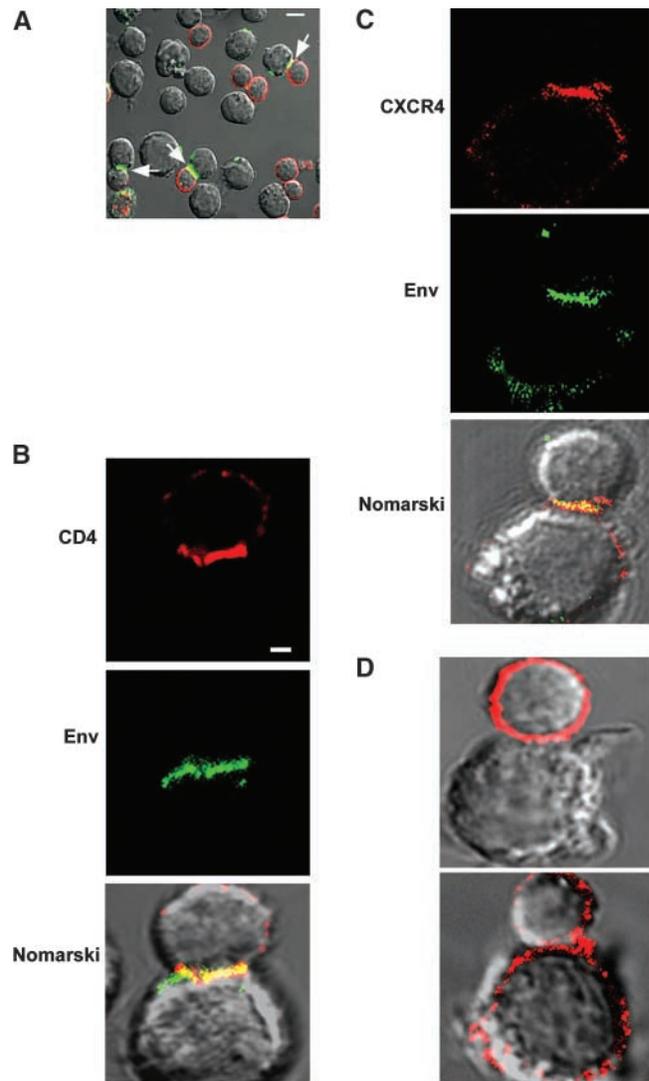

Figure 1.   Polarization of HIV-1 receptors and Env to the interface. Conjugates formed for 30 min between Jurkat$_{LAI}$ (effector) and primary CD4+ T (target) cells were labeled by indirect immunofluorescence, fixed, and analyzed by confocal microscopy. Images are single two-dimensional x-y sections through the central region of the cells with the corresponding Nomarski view of the cell surface. (A) Cells were stained during conjugate formation for CD4 (red) and gp41 (green) with mAbs L120 and 50-69, respectively. Conjugates with receptor-Env polarization and colocalization (yellow) are indicated with arrows. Bar, 10 μm. (B) Higher magnification of a target–effector cell conjugate showing polarized CD4 (red) and Env (green) colocalized (yellow) at the interface. Bar, 1 μm. (C) CXCR4 (red) on the target and effector cells copolarizes with Env (green) on the effector cell. (D) Conjugates between target cells and uninfected Jurkats do not show polarization of CD4 (top) or CXCR4 (bottom).

which six effector–target cell conjugates can be observed, of which three reveal polarized Env and CD4. One conjugate (Fig. 1 A, left) shows strong polarization of CD4 to the interface, whereas the other two have residual CD4 around the cell periphery. Env staining of unconjugated effector cells was often clustered into one or more patches on the cell surface (Fig. 1 A). This was not due to cross-linking of Env by the mAb during live cell 37°C staining because similar patching was observed when cells were stained on ice after conjugate formation or after fixation (unpublished data). Similarly, unconjugated target cells do not show any CD4 clustering, demonstrating that mAb alone is unable to cap CD4 (Fig. 1 B). Analysis of single conjugates at higher powers confirmed that CD4 (Fig. 1 B) frequently cocapped with Env at the interface. The polarization of CD4 to the interface varied from incomplete, where clustering at the interface was observed but residual receptor was distributed around the plasma membrane, to complete, when essentially all receptor was located at the interface (Figs. 1 B, 4 A, and 5, A and B).

Because we do not have CXCR4 mAbs that are non-blocking for the gp120–CXCR4 interaction, we stained for CXCR4 on ice in the presence of NaN$_3$ subsequent to arresting conjugate evolution. CXCR4 polarization was frequently observed on the target, and occasionally on the effector cell (Fig. 1 C). Because binding of the CXCR4 mAb was excluded by gp120–CXCR4 interactions, colocaliza-tion between CXCR4 and Env was generally less pronounced than that between CD4 and Env, although the frequency of CXCR4 polarization to the interface was similar to that observed for CD4. To rule out the possibility that receptor polarization was the result of interactions unrelated to Env expression, target cells conjugated with uninfected Jurkats were manipulated in the same way as for the cells in Fig. 1 (A–C). No CD4 or CXCR4 polarization was observed in the target cells under these conditions (Fig. 1 D).

Involvement of Adhesion and Other T Cell Surface Molecules. Interactions between the adhesion molecules LFA-1 and ICAM-1 increase HIV-1 infection and syncytium formation. Moreover, these interactions create an adhesive patch in immune cell interactions, which are intrinsic to formation of the immunological synapse (29). Therefore, we hypothesized that in a manner similar to the formation of an immunological synapse, LFA-1 might be recruited to the target–effector cell interface. We investigated the localization of the actin anchor protein talin and the associated integrin LFA-1 in conjugates. At 30 min, talin was observed in discrete microclusters at the interface of ~16% of conjugates, frequently forming partial ringlike structures (Fig. 2 A and unpublished data). LFA-1 was tightly associated with the interface and colocalized with Env (Fig. 2 B); because Jurkat$_{LAI}$ express little LFA-1, the clustering was clearly taking place on the target cell. No clustering of talin or LFA-1
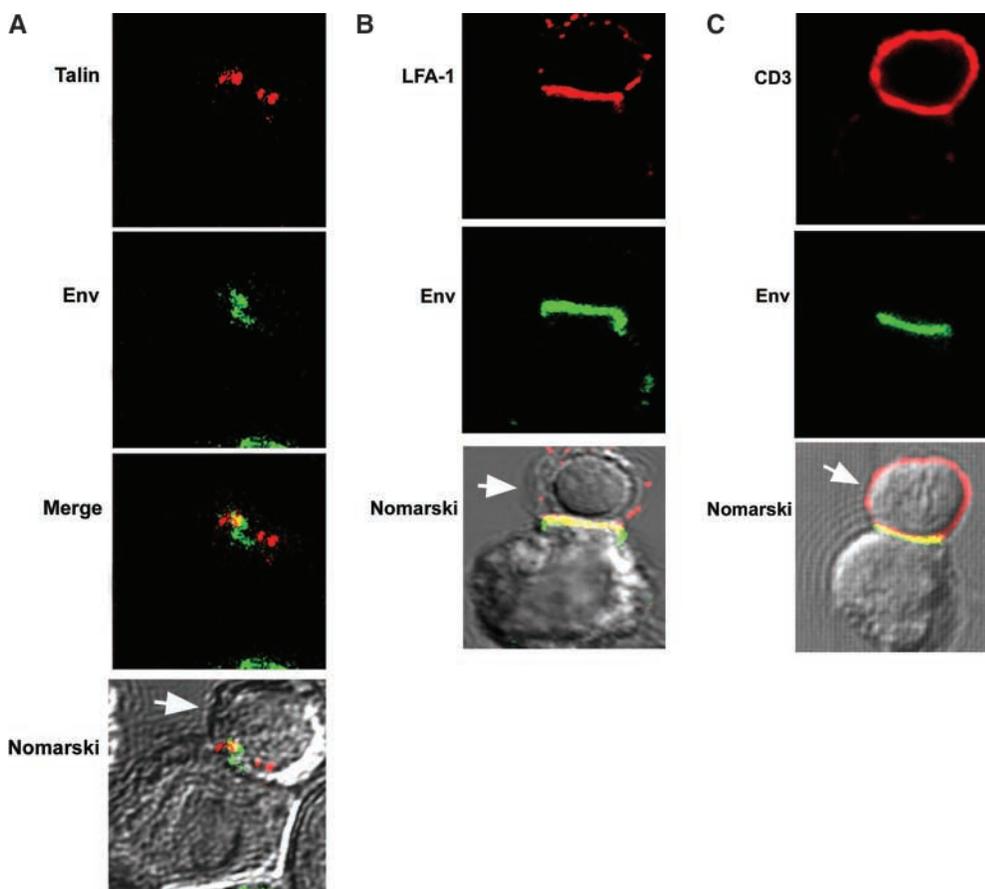

Figure 2. Talin and LFA-1 cluster at the target–effector cell interface. Conjugates between effector and target cells formed for 1 h at 37°C were stained for Env with 50-69 (green). The target cell was identified using a CD4-specific rabbit polyclonal serum (staining not depicted) and is indicated with an arrow. (A) Conjugates were either fixed with prechilled methanol and stained for the actin adaptor protein talin (red), (B) stained for the integrin LFA-1, or (C) CD3 before fixing in formaldehyde.
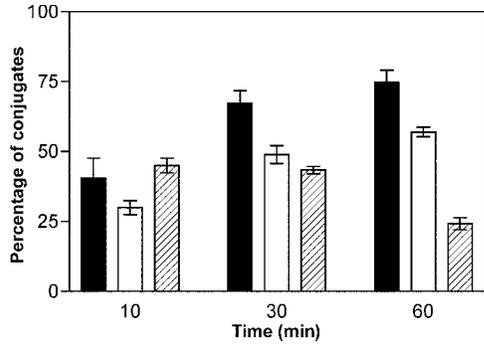
Figure 3. Kinetics of receptor polarization. Target and effector cells were mixed and incubated for 30 min on ice to synchronize cell adhesion to the poly-L-lysine–coated coverslips. Coverslips were transferred to 37°C and incubated for 10, 30, or 60 min before transfer to ice with the addition of NaN$_3$-containing buffer. Cells were either stained during conjugate formation with mAbs to Env and CD4 or to Env alone followed by incubation on ice to detect CD4 (using rabbit polyclonal serum), CXCR4, and LFA-1. Conjugates were fixed, stained with secondary antibodies, and analyzed by confocal microscopy. Conjugates were scored for copolarization of Env and CD4 (black bars), Env and LFA-1 (white bars), or polarization of CXCR4 alone (diagonally striped bars) The error bars show the standard error of the mean.

was observed on target cells in conjugates with uninfected Jurkats (unpublished data).

To assess the specificity of the molecular clustering, we stained 60-min conjugates for CD3. CD3 represents the T cell antigen receptor that is recruited into the immunological synapse. Despite tight clustering of Env at the interface, CD3 was generally not copolarized (Fig. 2 C), although ~15% of conjugates did show partial enrichment of CD3 at the interface. We conclude from these findings that Env ligation of the HIV receptors polarizes CD4, CXCR4, and LFA-1 to the interface and may partially enrich for other T cell markers.

Kinetics of CD4, CXCR4, and LFA-1 Recruitment. We estimated the rate of receptor and Env recruitment to the interface. Conjugate formation was synchronized at 4°C followed by 37°C for various times, after which cells were placed on ice, stained in the presence of NaN$_3$, fixed, and analyzed. Copolarization with Env was defined as cocapping of the molecules to the interface with little or no residual staining around the cell periphery as seen in Figs. 1, B and C, and 2 B. From a theoretical value of ~0%, CD4–Env copolarization at the interface at T = 0, copolarization was observed in ~40% of conjugates by 10 min, increasing

Table I. *Effect of Inhibitors on Conjugate Formation and Polarization*

Treatment	Conjugated[b]	Polarized[a]							
		CD4	CXCR4	Env	Gag	n[c]	Actin	n
	%	%	%	%	%	%	%	%
Untreated conjugates								
Jurkat$_{LAI}$ − CD4$^+$ cells	36	40	33	60	60	180	33	27
Jurkat − CD4$^+$ cells	11[d]	0	0	0	0	77	5	20
Blocking antibodies and receptor inhibitors								
Q4120	20[d]	0	ND[e]	0	0	68	4	81
447-52D	29[d]	0	ND	0	0	113	25	59
AMD3100	46	19	ND	15[d]	15[d]	86	9	54
Pharmacological inhibitors								
Cytochalasin D	17[d]	25[d]	0[d]	25[d]	25[d]	171	3[d]	171
Latrunculin	0	0	ND	0[d]	0[d]	65	0	36
Jasplakinolide	44	0	0[d]	0	0	75	ND	−
BDM	65[d]	20	0[d]	20	20	83	23[d]	59
ML7	63	16[d]	0[d]	13	13	69	20[d]	48
Wortmannin	100	14[d]	0[d]	14[d]	14[d]	51	22	64

Primary CD4$^+$ T cells were either untreated or pretreated with inhibitors before formation of conjugates with Jurkat$_{LAI}$. Cells were stained for CD4, CXCR4, Env, and Gagp17/p24 or CD4 and actin and analyzed by confocal microscopy for receptor polarization to the interface.
[a]The median percentage of primary CD4$^+$ T cells in conjugates with Jurkat$_{LAI}$ or uninfected Jurkat cells.
[b]The median percentage polarization was calculated by analyzing conjugates between Jurkat$_{LAI}$ or uninfected Jurkat and target primary CD4$^+$ T cells. Blocking antibodies and pharmacological inhibitors were applied as described in Materials and Methods.
[c]n indicates the number of primary cells examined from randomly chosen low power fields.
[d]Values do not differ significantly (P < 0.05) from the control (untreated Jurkat$_{LAI}$ − CD4$^+$ conjugates).
[e]ND, not done.

to 65% at 30 min and 75% at 60 min (Fig. 3). LFA–1 copolarization with Env was analyzed in the same manner. By 10 min, ~30% of LFA-1 was copolarized with Env, increasing to 50% at 30 min and 57% at 60 min. CXCR4 polarization was analyzed in the absence of coclustering with Env because the CXCR4 mAb does not bind gp120–CXCR4 complexes and, hence, did not consistently demonstrate strong colocalization between these molecules. Approximately 45% of conjugates had polarized CXCR4 staining at 10 min, decreasing to 42% at 30 min and 25% at 60 min. The decrease in CXCR4 staining was probably the result of progressive CXCR4 engagement by gp120, preventing binding of the detection mAb. This method of analysis overestimates the time required for receptor polarization because of the lag implicit in raising the temperature from 4 to 37°C, but demonstrates that receptor recruitment to the interface is a rapid and efficient process.

Requirement of the Env–Receptor Interaction For Receptor Clustering. To investigate the requirement of Env-CD4 and Env-CXCR4 engagement in receptor polarization, we inhibited these interactions and counted the number of conjugates formed and the percentage of conjugates containing copolarized CD4 and Env. For this, we prepared conjugates in the presence of mAb Q4120 that blocks CD4–gp120 interactions, 447-52D, a gp120 V3 loop-specific neutralizing mAb that blocks gp120–CXCR4 interac-

tions without interfering with gp120-CD4 binding, or AMD3100, a small molecule inhibitor of the gp120–CXCR4 interaction. At concentrations at which these inhibitors efficiently block HIV-1$_{LAI}$ infection, both mAbs reduced the frequency of conjugate formation and abolished CD4-Env polarization, whereas AMD3100 did not affect conjugate formation but reduced CD4 polarization significantly (Table I). Thus, both Env–CD4 and Env–CXCR4 interactions appear important in driving conjugate formation and inhibition of either is sufficient to interfere with CD4 recruitment.

Receptor Recruitment Requires the Actin Cytoskeleton. Recruitment of receptors and adhesion molecules into the immunological synapse is an actin-driven process (30). Suspecting that the rapid receptor polarization in our system might, therefore, require cytoskeletal remodeling, we stained conjugates for actin. Actin clustered in the target, but not the effector cell at the interface (Fig. 4 A) and colocalized partially with CD4 and Env. The percentage of conjugates containing polarized actin was significantly higher in the Jurkat$_{LAI}$–target cell conjugates than in the uninfected Jurkat–target conjugates (Table I). Moreover, inhibiting gp120–receptor interactions abolished (Q4210) or reduced (447-52D and AMD3100) actin polarization (Table I). These results imply that actin rearranges within the target cell in an Env-dependent manner.
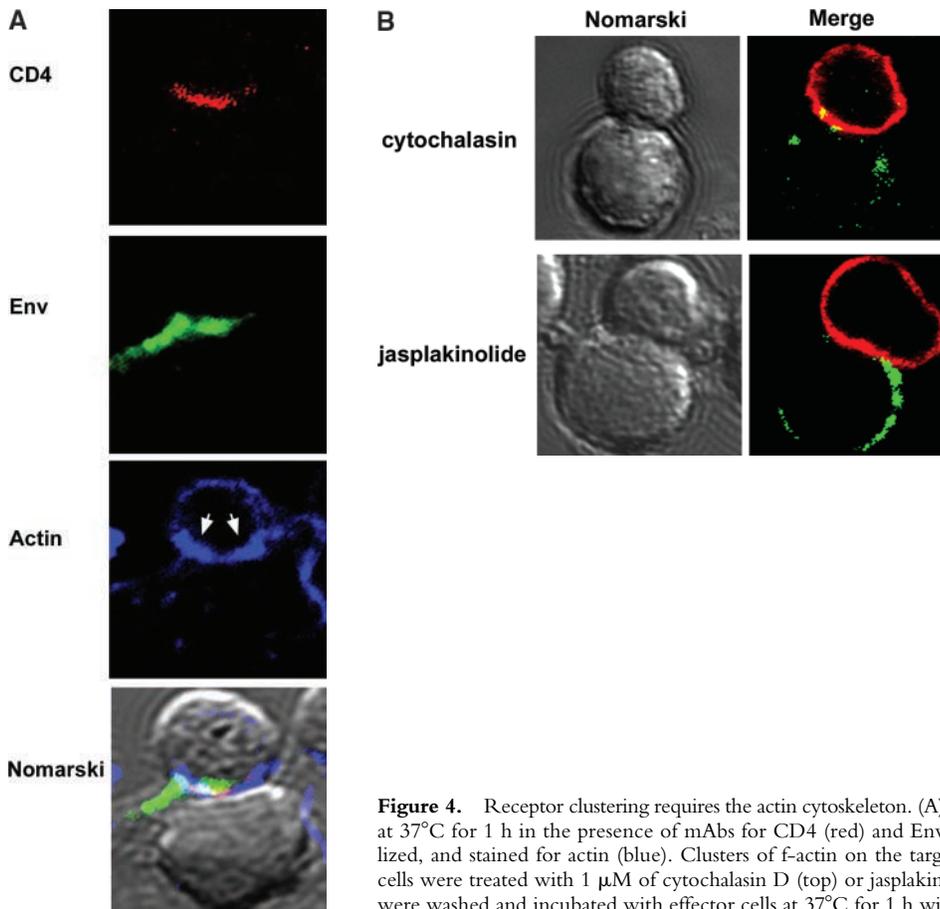

Figure 4. Receptor clustering requires the actin cytoskeleton. (A) Effector target cell conjugates were incubated at 37°C for 1 h in the presence of mAbs for CD4 (red) and Env (green). Conjugates were fixed, permeabilized, and stained for actin (blue). Clusters of f-actin on the target cell are indicated with arrows. (B) Target cells were treated with 1 µM of cytochalasin D (top) or jasplakinolide (bottom) for 1 h at 37°C. Treated cells were washed and incubated with effector cells at 37°C for 1 h with mAbs against CD4 (red) and Env (green).

To confirm or refute a role for actin in receptor polarization to the interface, we pretreated target cells with pharmacological inhibitors of actin remodelling. Cytochalasin D and latrunculin-A (31) depolymerize actin, whereas jasplakinolide (32) polymerizes and stabilizes actin. Target cells were pretreated with these inhibitors that were washed out before conjugate formation to prevent inhibition of actin remodelling in the effector cell. Cytochalasin D treatment reduced conjugate formation and CD4-Env polarization (Fig. 4 B and Table I), and actin polarization was inhibited by this treatment (not depicted), demonstrating that the inhibitor was functional. Incomplete inhibition of receptor recruitment by cytochalasin D probably reflects loss of inhibition over time after washing out. Treatment with latrunculin A, a more potent inhibitor than cytochalasin, completely blocked conjugate formation, suggesting that actin polymerization is essential for the formation of stable con-

tacts between target and effector cells. In contrast, jasplakinolide had no significant effect on conjugate formation but completely blocked CD4, CXCR4, and Env copolarization to the interface. Thus, paralyzing the actin cytoskeleton is sufficient to prevent receptor recruitment in this system.

The actin cytoskeleton can move via assembly and disassembly of actin filaments and by sliding filaments over one another using myosin motor proteins (33). To investigate the role of myosin motor–driven actin movement in receptor polarization, we used BDM, an inhibitor of myosin ATPase (33) and ML7, an inhibitor of myosin light chain kinase (34), to inhibit myosin motor function. Pretreatment of target cells with 20 mM BDM or 20 μM ML7 resulted in 50 and 60% reductions in CD4 polarization, respectively, interfered to a similar extent with Env polarization, and reduced actin polarization (Table I). CXCR4 recruitment was completely abolished by ML7
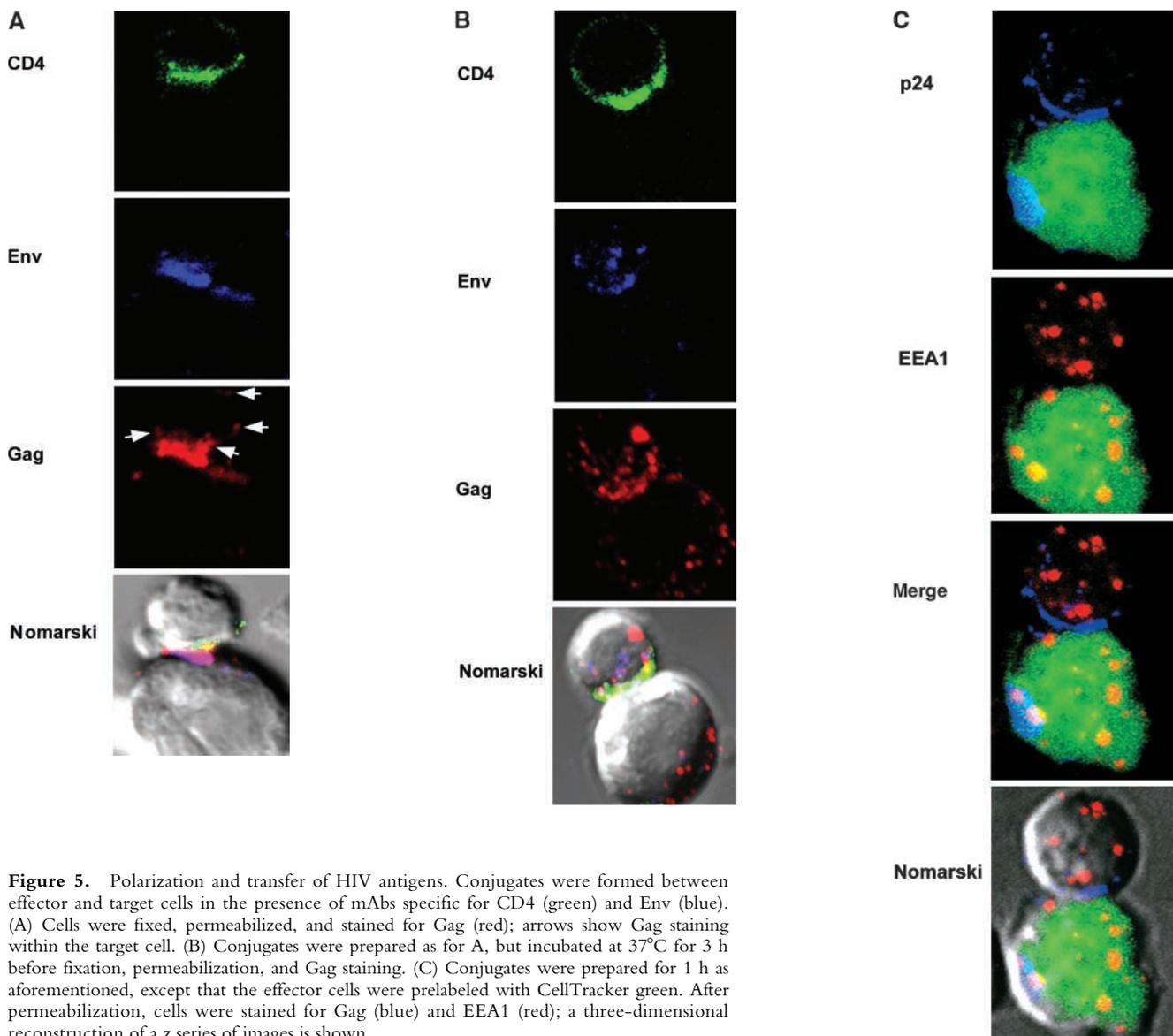

Figure 5. Polarization and transfer of HIV antigens. Conjugates were formed between effector and target cells in the presence of mAbs specific for CD4 (green) and Env (blue). (A) Cells were fixed, permeabilized, and stained for Gag (red); arrows show Gag staining within the target cell. (B) Conjugates were prepared as for A, but incubated at 37°C for 3 h before fixation, permeabilization, and Gag staining. (C) Conjugates were prepared for 1 h as aforementioned, except that the effector cells were prelabeled with CellTracker green. After permeabilization, cells were stained for Gag (blue) and EEA1 (red); a three-dimensional reconstruction of a z series of images is shown.

treatment of the target cells. Wortmannin inhibits myosin light chain kinase activity (35); this inhibitor increased conjugate formation by an unknown mechanism but significantly reduced CD4 and Env polarization. The incomplete block to receptor recruitment by these myosin motor inhibitors may reflect reversal of inhibition after washing out before conjugate formation or, alternatively, receptor movement may be mediated by a combination of actin depolymerization/repolymerization and myosin motor movement. Together, these data provide a compelling argument that actin rearrangement in the target cell is required for Env-driven receptor recruitment.

Polarization and Transfer of HIV-1 Gag and Env. The formation of adhesive junctions at the target–effector cell interface may facilitate HIV-1 infection. To investigate the movement of virus in our system, we analyzed conjugates for viral Gag and Env localization. Conjugates formed in the presence of mAbs L120 and 50-69 were fixed, permeabilized, and stained with antisera against Gag$^{p17/p24}$. Gag and Env frequently colocalized with CD4 at the interface, attaining a maximum level of clustering within 1 h (Fig. 5 A). Gag could be observed within the target cell from 1 h after conjugate initiation onwards (Fig. 5 A, arrows), demonstrating rapid and, by 3 h, massive (Fig. 5 B) translocation of viral core protein across the interface into the target cell. Env could also be seen located on and within the target cell, although to a lesser extent than Gag. At 1 h after conjugate formation, much of the Gag colocalized with Env at the interface. However, by 3 h, the majority of Gag was uncoupled from Env. The presence of Env stained with 50-69 on and in the target cell strongly suggests that Env-mediated fusion with the target cell has taken place, depositing Env in the target cell membrane and potentially leading to its subsequent internalization by endocytosis (36). To exclude the possibility that Gag and Env, possibly in the form of virions, were being taken into the target cell by endocytosis (a potentially nonproductive route of viral entry), we costained for Gag and EEA1, an early endosome marker. Fig. 5 C shows negligible colocalization between Gag^{p24} staining in the target cell and the EEA1 marker, strongly suggesting that most Gag enters cells via a nonendocytic route.

Inhibition of the interactions between CD4 or CXCR4 and Env by mAbs Q4120 and 447D prevented Gag clustering at the interface and transfer into the target cell coordinate with the lack of Env-receptor clustering (Table I). Inhibition of actin remodelling in the target cell using pharmacological inhibitors greatly reduced, and in the case of jasplakinolide, abolished Gag polarization and transfer (Table I). These data indicate that actin-dependent events, taking place in the target cell, are crucial for Gag recruitment from within the effector cell to the interface and its subsequent transfer into the target cell. We did not observe Gag or Env-positive target cells that were not conjugated with effectors, implying that cell to cell transfer, rather than cell-free virus, is responsible for virus entry into target cells.

The Mechanism of Gag Transfer into the Target Cell. One outcome of contact between HIV-1–infected and receptor-expressing target cells is cell–cell fusion. To establish whether cell–cell fusion was taking place under our experimental conditions, we labeled the target and effector cells with, respectively, green and red cytoplasmic dyes. These dyes do not leach out of the cells over time, so the detection of dye transfer in conjugates is good evidence of cytoplasmic exchange via fusion pores. Effector–target cell conjugates were formed and incubated at 37°C for up to 24 h. By 24 h after initiation of conjugate formation, dye transfer from effector to target cells was observed in ~80% of conjugates, although there was no evidence of syncytium formation, suggesting that cell–cell fusion in our system is inefficient. In contrast, dye transfer was not observed in any conjugates at 1, 3, or 6 h (Fig. 6 and not depicted). To ensure that the transfer was via gp41-mediated fusion, we incubated conjugates for 24 h in the presence of the gp41-derived fusion inhibitor DP178. Under these conditions, dye transfer was eliminated. The dramatic difference in the kinetics of Gag transfer and cell–cell fusion exclude the possibility that HIV movement from effector to target cells is via direct cell–cell fusion.

HIV-1 virions can bud in a directional manner between infected and uninfected cells (3). To investigate whether HIV-1 transfer from effector to target cells might occur in this way, we analyzed conjugates by TEM. Conjugates were formed by mixing equal numbers of effector and target cells at 37°C in the presence of L120. After fixation, cells labeled for CD4 were immunostained with gold particles. Fig. 7 shows the interface formed between an effector and a target cell after 1 h conjugate formation. Two regions of tight apposition between the cell plasma membranes are evident and virions with dense cores are observed at the interface and attached to the target cell membrane. Virions were not ob-
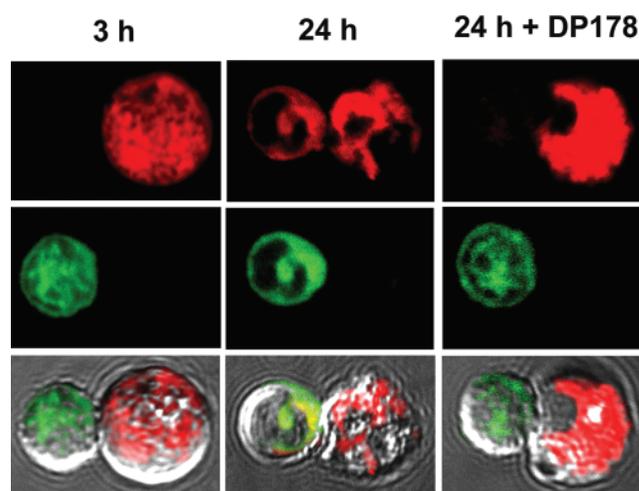

Figure 6. Kinetics of Env-mediated cell–cell fusion. Effector (red) and target (green) cells were labeled with cytoplasmic dyes, and conjugates were formed at 37°C in the presence or absence of DP178 for various times. The cells were fixed, and the conjugates were analyzed for fusion and mixing of cytoplasmic dyes (yellow). After 3 h of conjugate formation (left), no transfer of dye is detected; by 24 h, transfer of dye is apparent (middle) and this is blocked in conjugates formed for 24 h in the presence of DP178 (right).
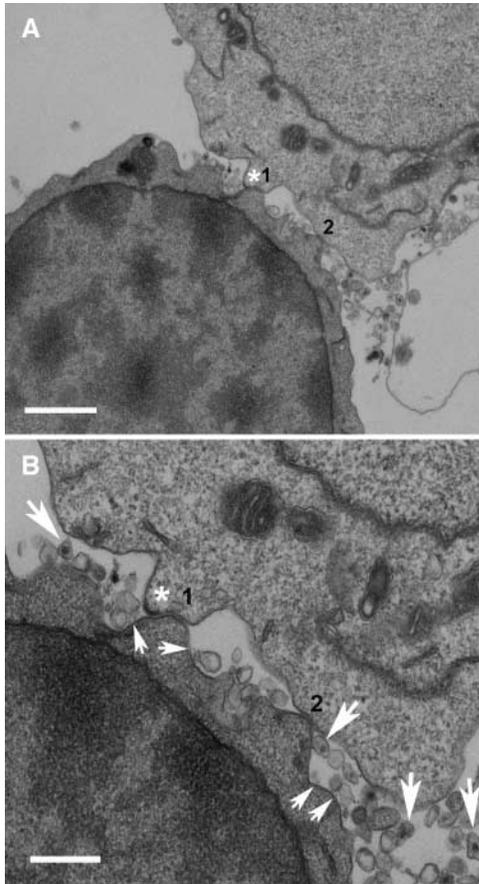
Figure 7. Immunoelectron microscopy showing clusters of HIV-1 particles at the synapse. Effector–target conjugates were formed for 1 h and processed for electron microscopy. (A) Low magnification (11,000×) of an ultrathin section through an effector–target cell conjugate. Closely apposed regions of membrane are numbered (1 and 2). Bar, 1 μm. (B) Higher magnification (30,000×) of the interface in the same conjugate. Small arrows highlight 6 nm of gold particles bound to CD4 on the target cell. Large arrows show mature virions associated with the membrane of the target cell, and the asterisk marks a structure resembling a budding virion. Bar, 300 nm.

served elsewhere on effector cell membranes, confirming clustering of virions at the interface (Fig. 7 A and not depicted). In Fig. 7 B, a structure resembling a virion budding from the effector cell membrane is shown, and gold particles labeling the target cell membrane are visible. In none of ∼50 conjugates examined by TEM have we observed evidence of endocytic uptake of virions into target cells.

Discussion

We have established a model system to study virus transfer between HIV-1–infected and uninfected T cells and have demonstrated that Env-dependent recruitment of CD4, CXCR4, and LFA-1 to the interface is via an actin-dependent mechanism probably involving myosin motor proteins. Adhesion molecule interactions play an important role in cell-free and cell–cell HIV-1 transmission (37), and

the active recruitment of LFA-1 on the target cell will increase intercellular adhesion via interactions with cognate partners on the effector cell, probably facilitating viral infection of the target cell. Therefore, we propose that cytoskeleton-dependent receptor movement associated with the formation of an adhesive junction provides an explanation for the high efficiency with which HIV-1 infects target cells by cell–cell transfer.

The directed transfer of material across an adhesive junction between two cells fits the definition of a synapse as described for neural and immunological synapses (38). We suggest that HIV induces a "virological synapse" between T cells by the formation and exploitation of an adhesive junction. Two other recent papers (2, 11) demonstrate related phenomena. One (11) demonstrates that DCs that have been pulsed with HIV-1 focus the virus at the interface with CD4$^+$ T cells to allow efficient infection of the target cells. Similar to our paper, they propose that the viral receptors and infectious virus particles are corecruited to the DC–T cell interface, although they do not elucidate the mode of recruitment. The other work (2) describes a model in which HTLV-1 moves from infected to uninfected T cells. This latter paper characterizes synapse formation predominantly in the HTLV-1–infected cell. Because the HTLV-1 receptors are unknown, recruitment cannot at present be analyzed, and the role of viral Env is unclear. Together with our results, it seems likely that the ability to form synapselike structures may be generalizable to other viruses with the caveat that viral engagement of cell surface receptors should induce cytoskeletal movement required to drive synapse formation. There may also be parallels between actin-dependent cell–cell spread of viruses and actin-mediated uptake of other pathogens, such as bacteria (39) and parasites (40).

We used an X4, T cell line–adapted virus in Jurkat cells as the effector cell. Cell line adaptation leads to modification of the properties of Env compared with primary isolate virus, such as increased CD4 affinity and neutralization sensitivity (41). However, these changes appear to be more quantitative than qualitative, and we believe that the virus we have used here reflects the general properties of HIV-1 X4 Env. In support of this, preliminary results using a primary isolate R5X4 dual-tropic HIV-1 (89.6) are similar to those we report here for the LAI isolate (unpublished data). Our model uses primary CD4$^+$/CXCR4$^+$ target T cells. Although X4 viruses appear later in infection than R5 viruses and are detected in only ∼50% HIV-1–infected individuals, they are associated with rapid progression of the infection and increased depletion of CD4$^+$ T cells. Despite the obvious relevance of X4 HIV-1 isolates to HIV-1 disease, it will nevertheless be important to establish whether CCR5-tropic virus-infected T cells can induce similar synaptic structures in CD4$^+$/CCR5$^+$ T cells.

What are the molecular mechanisms underlying the formation of an HIV-1–induced T cell synapse? The observation that inhibitors of the CD4–gp120 and CXCR4–gp120 interactions prevent or reduce actin-mediated receptor polarization supports their central role. Interference with po-

larization of Env and Gag by paralyzing the actin cytoskeleton in target cells implies that CD4 and CXCR4 are the molecules driving Env-Gag recruitment to the interface rather than the inverse. Therefore, we hypothesize that initial cross-linking of small numbers of CD4 and CXCR4 molecules by membrane-associated Env or cell surface–associated virions induces reorganization of the actin cytoskeleton that recruits more receptors, along with talin and LFA-1, to the interface. Links between actin and CD4 (42) and CXCR4 (43) have been proposed, and integrins such as LFA-1 associate with actin via anchor proteins such as talin, and their clustering is actin mediated (44). Moreover, both CD4 and CXCR4 cluster within actin- and lipid raft–rich microvilli on human T cells (45, 46), and lipid rafts may associate with actin (47). The mechanism by which actin mediates CD4, CXCR4, and LFA-1 movement remains to be elucidated, but may involve signaling induced by Env engagement of either, or both, CD4 and CXCR4 (48, 49).

We have demonstrated that HIV-1 Gag moves across the synaptic junction into the target cell in 1–3 h. Although we have not formally demonstrated that Gag transfer corresponds to productive infection, previous papers demonstrate unequivocally that productive infection of T cells by cell–cell spread of HIV-1 takes place within a similar time frame (5, 12). We did not detect evidence of cell–cell fusion until 24 h after conjugate formation. This confirms that passage of viral Gag via fusion pores is most unlikely to be the mode of transfer that we observe, in accord with other studies of cell–cell HIV-1 spread (3). Our inability to detect syncytium formation and cell–cell fusion within 6 h contrasts with other analyses of HIV-1 Env-mediated cell–cell fusion (20, 23). Such differences in kinetics probably result from our use of resting primary T cells as targets rather than activated or immortalized T cells; quiescent T cells are less fusogenic because they lack activated adhesion molecules and potentially other cell surface structures upregulated upon T cell activation or transformation.

Our TEM analysis of effector–target cell conjugates reveals regions of close packing of effector and target cell plasma membranes with virus particles concentrated in this region. Polarized viral budding has been observed at sites of contact between HIV-infected and uninfected cells by others, during which virions produced at the interface are thought to enter target cells via fusion with the plasma membrane (3). These data, together with our TEM and confocal analyses, strongly imply that HIV-1 particles cluster at the effector–target cell interface in a "synaptic space," across which virions fuse with the target cell membrane.

In conclusion, we have described a novel system for the study of cell–cell dissemination of HIV-1 that may help to explain the rapid movement of virus between permissive cells. Further study of the HIV-1–induced virological synapse will help to elucidate strategies to interfere with this mode of virus spread.

References

1. Johnson, D., and M. Huber. 2002. Directed egress of animal viruses promotes cell-to-cell spread. *J. Virol.* 76:1–8.
2. Igakura, T., J. Stinchcombe, P. Goon, G. Taylor, J. Weber, G. Griffiths, Y. Tanaka, M. Osame, and C. Bangham. 2003. Spread of HTLV-1 between lymphocytes by virus-induced polarisation of the cytoskeleton. *Science.* 299:1713–1716.
3. Phillips, D. 1994. The role of cell-to-cell transmission in HIV infection. *AIDS.* 8:719–731.
4. Haase, A. 1999. Population biology of HIV-1 infection: viral and CD4+ T cell demographics and dynamics in lymphatic tissue. *Annu. Rev. Immunol.* 17:625–656.
5. Sato, H., J. Orenstein, D. Dimitrov, and M. Martin. 1992. Cell-cell spread of HIV-1 occurs within minutes and may not involve the participation of virus particles. *Virology.* 186:712–724.
6. Fais, S., M. Capobianchi, I. Abbate, C. Castilletti, M. Gentile, P. Fei, F. Ameglio, and F. Dianzani. 1995. Unidirectional budding of HIV-1 at the site of cell-to-cell contact is associated with co-polarization of intercellular adhesion molecules and HIV-1 viral matrix protein. *AIDS.* 9:329–335.
7. Phillips, D., and A. Bourinbaiar. 1992. Mechanism of HIV spread from lymphocytes to epithelia. *Virology.* 186:261–273.
8. Phillips, D., X. Tan, M.-E. Perotti, and V. Zacharopoulos. 1998. Mechanism of monocyte-macrophage-mediated transmission of HIV. *AIDS Res. Hum. Retroviruses.* 14:S67–S70.
9. Pope, M., M. Betjes, N. Romani, H. Hirmand, P. Cameron, L. Hoffman, S. Gezelter, G. Schuler, and R. Steinman. 1994. Conjugates of dendritic cells and memory T lymphocytes from skin facilitate productive infection with HIV-1. *Cell.* 89:389–398.
10. Tsunetsugu-Yokota, Y., S. Yasuda, A. Sugimoto, T. Yagi, M. Azuma, H. Yagita, K. Akagawa, and T. Takemori. 1997. Efficient virus transmission from dendritic cells to CD4+ T cells in response to antigen depends on close contact through adhesion molecules. *Virology.* 239:259–268.
11. McDonald, D., L. Wu, S. Bohks, V. KewalRamani, D. Unutmaz, and T. Hope. 2003. Recruitment of HIV and its receptors to dendritic cell-T cell junctions. *Science.* 300:1295–1297.
12. Davis, A., P. Li, and C. Burrell. 1997. Kinetics of viral RNA synthesis following cell-to-cell transmission of human immunodeficiency virus type 1. *J. Gen. Virol.* 78:1897–1906.
13. Berger, E.A. 1997. HIV entry and tropism: the chemokine receptor connection. *AIDS.* 11:S3–S16.
14. Moore, J.P., A. Trkola, and T. Dragic. 1997. Co-receptors for HIV-1 entry. *Curr. Opin. Immunol.* 9:551–562.
15. Layne, S.P., M.J. Merges, M. Dembo, J.L. Spouge, and P.L. Nara. 1990. HIV requires multiple gp120 molecules for CD4-mediated infection. *Nature.* 346:277–279.
16. Moore, J.P., J.A. McKeating, W.A. Norton, and Q.J. Sattentau. 1991. Direct measurement of soluble CD4 binding to human immunodeficiency virus type 1 virions: gp120 dissociation and its implications for virus-cell binding and fusion reactions and their neutralisation by soluble CD4. *J. Virol.* 65:1133–1140.
17. Kuhmann, S.E., E. Platt, S. Kozak, and D. Kabat. 2000. Co-

operation of multiple CCR5 coreceptors is required for infections by human immunodeficiency virus type 1. *J. Virol.* 74:7005–7015.

18. Doms, R. 2000. Beyond receptor expression: the influence of receptor conformation, density, and affinity in HIV-1 infection. *Virology.* 276:229–273.

19. Iyengar, S., J. Hildreth, and D. Schwartz. 1998. Actin-dependent receptor colocalisation required for human immunodeficiency virus entry into host cells. *J. Virol.* 72:5251–5255.

20. Frey, S., M. Marsh, A. Pelchen-Matthews, P. Stephens, S. Ortlepp, and T. Stegmann. 1995. Temperature-dependence of cell–cell fusion induced by the envelope glycoprotein of human immunodeficiency virus type 1. *J. Virol.* 69:1462–1472.

21. Dimitrov, D., and R. Blumenthal. 1994. Photoinactivation and kinetics of membrane fusion mediated by the human immunodeficiency virus type 1 envelope glycoprotein. *J. Virol.* 68:1956–1961.

22. Jones, P.L.S.J., T. Korte, and R. Blumenthal. 1998. Conformational changes in cell surface HIV-1 envelope glycoproteins are triggered by cooperation between cell surface CD4 and coreceptors. *J. Biol. Chem.* 273:404–409.

23. Markosyan, R., F. Cohen, and G. Melikyan. 2003. HIV-1 envelope proteins complete their folding into six helix bundles immediately after fusion pore formation. *Mol. Biol. Cell.* 14:926–938.

24. Healey, D., L. Dianda, J.P. Moore, J.S. McDougal, M.J. Moore, P. Estess, D. Buck, P.D. Kwong, P.C.L. Beverley, and Q.J. Sattentau. 1990. Novel anti-CD4 monoclonal antibodies separate human immunodeficiency virus infection and fusion of CD4$^+$ cells from virus binding. *J. Exp. Med.* 172:1233–1242.

25. Sattentau, Q.J., and J.P. Moore. 1991. Conformational changes induced in the human immunodeficiency virus envelope glycoproteins by soluble CD4 binding. *J. Exp. Med.* 174:407–415.

26. Mondor, I., M. Moulard, S. Ugolini, P.-J. Klasse, J. Hoxie, R. Wyatt, J. Sodroski, and Q.J. Sattentau. 1998. Interactions between HIV gp120, CD4 and CXCR4: dependence on CD4 expression level, viral origin of gp120, conservation of the gp120 COOH and NH2-termini and V1V2 and V3 loops, and sensitivity to neutralizing antibodies. *Virology.* 248:394–432.

27. Conley, A.J., M.K. Gorny, J.A. Kessler II, L.J. Boots, M. Ossorio-Castro, S. Koenig, D.W. Lineberger, E.A. Emini, C. Williams, and S. Zolla-Pazner. 1994. Neutralization of primary human immunodeficiency virus type 1 isolates by the broadly reactive anti-V3 monoclonal antibody, 447-52D. *J. Virol.* 68:6994–7000.

28. Kilby, J., S. Hopkins, T. Venetta, B. DiMassimo, G. Cloud, J. Lee, L. Alldrege, E. Hunter, D. Lambert, D. Bolognesi, T. Matthews, M. Johnson, M. Nowak, G. Shaw, and M. Saag. 1998. Potent suppression of HIV-1 replication in humans by T-20, a peptide inhibitor of gp41-mediated virus entry. *Nature Med.* 4:1302–1307.

29. Krummel, M., and M. Davis. 2002. Dynamics of the immunological synapse: finding, establishing and solidifying a connection. *Curr. Opin. Immunol.* 14:66–74.

30. Dustin, M., and J. Cooper. 2000. The immunological synapse and the actin cytoskeleton: molecular hardware for T cell signaling. *Nat. Immunol.* 1:23–29.

31. Spector, I., N. Shochet, D. Blasberger, and Y. Kashman. 1989. Latrunculins-novel marine macrolides that disrupt microfilament organisation and affect cell growth: I comparison with Cytochalasin D. *Cell Motil. Cytoskeleton.* 13:127–144.

32. Bubb, M., A. Senderowicz, E. Sausville, K. Duncan, and E. Korn. 1994. Jasplakinolide, a cytotoxic natural product, induces actin polymerisation and competitively inhibits the binding of phalloidin to F-actin. *J. Biol. Chem.* 269:14869–14871.

33. Mitchison, T., and L. Cram. 1996. Actin-based cell motility and cell locomotion. *Cell.* 84:371–379.

34. Saitoh, M., T. Ishikawa, S. Matsushima, M. Naka, and H. Hidaka. 1987. Selective inhibition of catalytic activity of smooth muscle myosin light-chain kinase. *J. Biol. Chem.* 262:7796–7801.

35. Nakanishi, S., K. Catt, and T. Balla. 1994. Inhibition of agonist-stimulated inositol 1,4,5-triphosphate production and calcium signalling by the myosin light chain kinase inhibitor, wortmannin. *J. Biol. Chem.* 269:6528–6535.

36. West, J.T., S.K. Weldon, S. Wyss, X. Lin, Q. Yu, M. Thali, and E. Hunter. 2002. Mutation of the dominant endocytosis motif in human immunodeficiency virus type 1 gp41 can complement matrix mutations without increasing Env incorporation. *J. Virol.* 76:3338–3349.

37. Tremblay, M.J., J.-F. Fortin, and R. Cantin. 1998. The acquisition of host-encoded proteins by nascent HIV-1. *Immunol. Today.* 19:346–351.

38. Dustin, M., and D. Colman. 2002. Neural and immunological synaptic relations. *Science.* 298:785–789.

39. Hayward, R., and V. Koronakis. 2002. Direct modulation of the host cell cytoskeleton by *Salmonella* actin-binding proteins. *Trends Cell Biol.* 12:15–20.

40. Sibley, L., and N. Andrews. 2000. Cell invasion by un-palatable parasites. *Traffic.* 1:100–106.

41. Moore, J.P., and D.D. Ho. 1995. HIV neutralization: the consequence of viral adaptation to growth on transformed T cells. *AIDS.* 9(Suppl.):S117–S136.

42. Kinch, M., J. Strominger, and C. Doyle. 1993. Cell adhesion mediated by CD4 and MHC class-II proteins requires active cellular processes. *J. Immunol.* 151:4552–4561.

43. Rey, M., M. Vicente-Manzanares, F. Viedma, M. Yanez-Mo, A. Urzainqui, O. Barreiro, J. Vazquez, and F. Sanchez-Madrid. 2002. Cutting edge: association of the motor protein nonmuscle myosin heavy chain-IIA with the C terminus of the chemokine receptor CXCR4 in T lymphocytes. *J. Immunol.* 169:5410–5414.

44. Schoenwalelder, S., and K. Burridge. 1999. Bidirectional signalling between the cytoskeleton and integrins. *Curr. Opin. Cell Biol.* 11:274–286.

45. Singer, I., S. Scott, D. Kawka, J. Chin, B. Daugherty, J. DeMartino, J. DiSalvo, S. Gould, J. Lineberger, L. Malkowitz, et al. 2001. CCR5, CXCR4 and CD4 are clustered and closely apposed on microvilli of human macrophages and T cells. *J. Virol.* 75:3779–3790.

46. Foti, M., M.-A. Phelouzat, A. Holm, B. Rasmusson, and J.-L. Carpentier. 2002. p56lck anchors CD4 to distinct microdomains on microvilli. *Proc. Natl. Acad. Sci. USA.* 99:2008–2013.

47. Harder, T., R. Kellner, R. Parton, and J. Gruenberg. 1997. Specific release of membrane-bound annexin-II and cortical cytoskeletal elements by sequestration of membrane cholesterol. *Mol. Biol. Cell.* 8:533–545.

48. Davis, C.B., I. Dikic, D. Unutmaz, C.M. Hill, J. Arthos, M.A. Siani, D.A. Thompson, J. Schlessinger, and D.R. Littman. 1997. Signal transduction due to HIV-1 envelope interactions with chemokine receptors CXCR4 or CCR5. *J. Exp. Med.* 186:1793–1798.

49. Kinter, A., A. Catanzaro, J. Monaco, M. Ruiz, J. Justement, S. Moir, J. Arthos, A. Oliva, L. Ehler, S. Mizell, et al. 1998. CC-chemokines enhance the replication of T-tropic strains of HIV-1 in CD4(+) T cells: role of signal transduction. *Proc. Natl. Acad. Sci. USA.* 95:11880–11885.